

---

# COPT: Coordinated Optimal Transport on Graphs

---

Yihe Dong<sup>1</sup> Will Sawin<sup>2</sup>

## Abstract

We introduce COPT, a novel distance metric between graphs defined via an optimization routine, computing a coordinated pair of optimal transport maps simultaneously. This is an unsupervised way to learn general-purpose graph representations, it can be used for both graph sketching and graph comparison. COPT involves simultaneously optimizing dual transport plans, one between the vertices of two graphs, and another between graph signal probability distributions. We show both theoretically and empirically that our method preserves important global structural information on graphs, in particular spectral information, making it well-suited for tasks on graphs including retrieval, classification, summarization, and visualization.

## 1. Introduction

We introduce a new unsupervised method to sketch graphs, and to measure the distance between a pair of graphs. We explain the distance function first, which the sketching method is based on. This distance is based on the general notion of optimal transport distance, which involves minimizing a loss function over transport plans between two distributions (Kantorovich, 1942). However, our distance is defined by minimizing a loss function over *pairs* of simultaneous transport plans, one between the vertices of the two graph and one between distributions defined by the Laplacian spectra of the graphs. This allows us to compare, in a flexible way, large-scale spectral information between the two graphs. Thus, we call it COordinated Optimal Transport, or COPT.

We show that this distance can be used effectively for graph retrieval, as judged by nearest-neighbor based classification accuracy. The search dataset consists of different classes of randomly generated graphs, and the task is to correctly classify a query graph by using the class of its nearest neighbor in the dataset.

By combining COPT distance with the state of the art

Gromov-Wasserstein (GW) distance – a distance for graphs defined using optimal transport (Mémoli, 2011; Peyré et al., 2016; Vayer et al., 2019), we are able to consistently improve performance on graph classification than using GW alone. We justify this as due to the fact that COPT measures large-scale spectral information of the graph, while GW distance measures large-scale metric information of the graph, and thus combining them gives a more complete picture of the graph structure than either alone.

We subsequently define a sketch procedure which is based on finding the closest low-dimensional approximation in our coordinated optimal transport distance. We show that COPT is able to sketch insightful graph visualizations that are useful both for distilling the key structures within a graph, as well as revealing relations amongst graphs, when sketched to three dimensions.

Another relevant application of sketching is illustrated by using sketched graph Laplacians as uniformized, low-dimensional, high-fidelity vector representations of the original graphs. Returning to the classification problem, by vectorizing the search dataset with COPT sketching, we are able to achieve high classification accuracy – a significant boost over spectral projections of the original graphs, all whilst being computationally efficient, for instance over  $2000\times$  faster than GW.

Our **main contributions** are: 1) devising a coordinated optimal transport algorithm for computing graph distance; 2) applying COPT to graph sketching, obtaining small sketches that allow for insightful visualizations and high retrieval quality; 3) obtaining improvements, when combined with state of the art methods, on graph classification problems.

COPT has the flexibility to sketch graphs of varying cardinalities down to uniform cardinalities. Uniformized graphs can be more easily adapted for downstream tasks such as neural network training without additional processing such as padding, where batching is standard practice. Uniform data fit into contiguous equal-sized blocks of memory, enabling fast retrieval of large-scale data from disk as the access address can be computed as a simple offset.

We make more detailed comparisons with prior work throughout the text, here we highlight some recent developments in this field. Graph sketching is an important problem,

<sup>1</sup>Microsoft <sup>2</sup>Columbia University.

and a variety of approaches to it have appeared in the literature. (Ron et al., 2011) used iterated graph sketching to find optimal orderings of the vertices of a graph. (Chen & Safro, 2011) built on this to define an efficiently computable notion of distance on graphs. (Livne & Brandt, 2012) used sketching to efficiently solve linear systems involving the graph Laplacian. (Dörfler & Bullo, 2013) defined a sketch as the Schur complement of the Laplacian with respect to a subset of the nodes. (D. I. Shuman & Vandergheynst, 2016) generalized multiscale methods to graphs with extra structure on the nodes. (Loukas & Vandergheynst, 2018) simplified graphs by contracting edges in such a way as to preserve the Laplacian spectrum. (Bravo-Hermesdorff & Gunderson, 2019) remove edges and merge vertices in a way that minimizes the Frobenius norm of changes in the pseudoinverse of the Laplacian.

This paper is outlined as follows: In Section §2, we review generalities on optimal transport methods for graph comparison and discuss prior work. In Section §3, we define coordinated optimal transport distance and discuss its properties. In Section §4, we describe our approach to graph sketching. In Section §5, we discuss algorithm implementations and experimental results.

## 2. Graph distances based on optimal transport of vertices

In general, we would like a notion of “distance” for graphs that satisfies the properties of a metric, and in particular is zero if and only if the two graphs are isomorphic. We would also like this distance to be reasonably computable in practice.

Because no simple complete invariant for graphs up to isomorphism is known, the most natural approach to define a distance for graphs up to isomorphism is to define the distance between graphs  $X$  and  $Y$  as a minimum, over bijections between the vertices of  $X$  and the vertices of  $Y$ , of some quantity, which vanishes if and only if this bijection sends the edges of  $X$  to the edges of  $Y$ . For instance, we could take the minimum over bijections of the cardinality of the symmetric difference of the edge set. However, there are some downsides to minimizing over permutations.

First, such a distance would be hard to compute, or even approximate, in practice, as it involves a complicated discrete optimization problem.

Second, such a distance would not be defined if our graphs  $X$  and  $Y$  have different numbers of vertices.

To solve these problems, we can define a graph distance as a minimization over transport plans. To define these, we first **fix some notation**. Let  $X$  be a graph with  $N$  vertices and  $Y$  a graph with  $M$  vertices. We will also use  $X$  and

$Y$  to denote the set of vertices of  $X$  and  $Y$  respectively. Optimal transport plans are functions  $P$  from  $X \times Y$  to  $\mathbb{R} \cup \{0\}$  such that  $\sum_{x \in X} P(x, y) = N$  for all  $y \in Y$ , and  $\sum_{y \in Y} P(x, y) = M$  for all  $x \in X$ . We will define distances as a minimum over transport plans  $P$ , so their formulations will be analogous to the optimal transport, or Wasserstein, distance, defined as

$$W_p(X, Y) = \min_{\substack{P: X \times Y \rightarrow \mathbb{R}^+ \\ \sum_{x \in X} P(x, y) = N \\ \sum_{y \in Y} P(x, y) = M}} \left( \sum_{x \in X} \sum_{y \in Y} d(x, y)^p P(x, y) \right)^{1/p} \quad (1)$$

where  $d(x, y)$  is a distance function between two points.

**Gromov-Wasserstein distance.** However, before being able to apply (1), there is no notion of  $d(x, y)$  for  $x, y$  vertices in two different graphs.

To fix this, Mémoli proposed a notion of Gromov-Wasserstein distance for graphs (Mémoli, 2011), as the  $p$ th root of

$$\min_{\substack{P: X \times Y \rightarrow \mathbb{R}^+ \\ \sum_{x \in X} P(x, y) = N \\ \sum_{y \in Y} P(x, y) = M}} \sum_{\substack{x_1, x_2 \in X \\ y_1, y_2 \in Y}} L(x_1, x_2, y_1, y_2) P(x_1, y_1) P(x_2, y_2) \quad (2)$$

where

$$L(x_1, x_2, y_1, y_2) = (d_X(x_1, x_2) - d_Y(y_1, y_2))^p. \quad (3)$$

In other words, given the distance  $d_X$  for two vertices in the same graph, defined as the minimum number of edges in a path connecting them, we have a natural notion of distance between two pairs  $x_1, x_2$  and  $y_1, y_2$  of vertices on the two different graphs as the difference between the distances of the individual vertices.

A generalization of this definition to arbitrary functions  $L$ , along with computational methods and applications, was provided by (Peyré et al., 2016), building on computational ideas of (Cuturi, 2013). An application to word embeddings was given by (Alvarez-Melis & Jaakkola, 2018). A similar approach, but based more closely on Gromov-Hausdorff distance, was due to Sturm (Sturm, 2006).

**Graph Optimal Transport.** (Maretić et al., 2019) proposed GOT, a graph distance that uses optimal transport in a different way. This relies on a probability distribution  $\mu^X$ , the *graph signal* of  $X$  (Rue & Held, 2005; Dong et al., 2019), over functions on the vertices of  $X$ . This distribution is a multivariate Gaussian, with mean zero, whose variance-covariance matrix is a pseudo-inverse  $L_X^\dagger$  of the Laplacian  $L_X$ . They then define, in the case  $N = M$ , a distance for graphs defined by optimal transport of these probability distributions. Let  $T: \mathbb{R}^X \rightarrow \mathbb{R}^Y$  denote a transport plan and  $\sigma: X \rightarrow Y$  a permutation, (Maretić et al., 2019) defines a

distance as

$$W_2(\mu^X, \mu^Y)^2 \quad (4)$$

$$= \min_{\substack{\sigma: X \rightarrow Y \\ \sigma \text{ bijective}}} \inf_{\substack{T: \mathbb{R}^X \rightarrow \mathbb{R}^Y \\ T_{\#} \mu^X = \mu^Y}} \int_{\mathbb{R}^X} \sum_{x \in X} (f(x) - Tf(\sigma(x)))^2 d\mu^X(f)$$

### 3. Coordinated optimal transport

Our definition of a new metric on graphs builds on (4), where we replace the permutation  $\sigma$  with an optimal transport plan  $P$ . Thus, our definition involves two different optimal transport plans:  $P, T$ , hence named *coordinated optimal transport*. We define our distance  $\Delta(X, Y)$  by

$$NM\Delta(X, Y)^2 = \min_{\substack{P: X \times Y \rightarrow \mathbb{R}^+ \\ \sum_{x \in X} P(x, y) = N \\ \sum_{y \in Y} P(x, y) = M}} \inf_{\substack{T: \mathbb{R}^X \rightarrow \mathbb{R}^Y \\ T_{\#} \mu^X = \mu^Y}} L_{X, Y}(P, T) \quad (5)$$

where

$$L_{X, Y}(P, T) = \int_{\mathbb{R}^X} \sum_{x \in X} \sum_{y \in Y} (f(x) - Tf(y))^2 P(x, y) d\mu^X(f).$$

Again, we take  $\mu^X$  to be a Gaussian with mean zero and variance-covariance matrix  $L_X^\dagger$ .

In the special case that  $N = M$  and  $P$  is a permutation, this definition reduces to the definition in (Maretic et al., 2019), up to a normalization factor of  $\sqrt{N}$ . COPT is more general and can be used between graphs of different cardinalities and for sketching.

#### 3.1. Properties of COPT

We give an analytic formula for computing COPT distance  $\Delta(X, Y)$ , and show  $\Delta(X, Y)$  is a metric. See the supplementary material for full proofs.

**Lemma 3.1.** *Let  $X$  and  $Y$  be graphs with vertex sets of size  $N$  and  $M$  respectively. Then*

$$\inf_{\substack{T: \mathbb{R}^X \rightarrow \mathbb{R}^Y \\ T_{\#} \mu^X = \mu^Y}} \int_{\mathbb{R}^X} \sum_{x \in X} \sum_{y \in Y} (f(x) - Tf(y))^2 P(x, y) d\mu^X(f)$$

$$= M \operatorname{tr}(L_X^\dagger) + N \operatorname{tr}(L_Y^\dagger) - 2 \operatorname{tr}(((L_Y^\dagger)^{1/2} P^T L_X^\dagger P (L_Y^\dagger)^{1/2})^{1/2}) \quad (6)$$

where  $P$  is the matrix with entries  $P(x, y)$ .

*Proof summary.* We extend  $\mu^X$  and  $\mu^Y$  to distributions on the space of functions on  $X \times Y$ , in such a way that the infimum we are interested in is exactly the Wasserstein distance between these distributions. Because the extended distributions remain multivariate Gaussians, we can use the known Wasserstein distance formula for multivariate Gaussians (Takatsu, 2011). By calculating the variance of these

extended distributions, and using the cyclic permutation invariance of the traces of powers of a matrix, this reduces to our stated formula.  $\square$

Using this analytic formula for the minimum over  $T$ , we can approximate the coordinated optimal transport distance by using gradient descent to handle the minimum only over  $P$ .

**Lemma 3.2.**  $\Delta(X, Y)$  is a metric on the set of isomorphism classes of finite graphs.

*Proof summary.* We check each axiom from the definition of a metric separately. For each of them, our strategy is based on the corresponding step in the proof that the Wasserstein distance is a metric. Whatever construction must be applied to the transport map or joint measure in the Wasserstein distance proof is applied to both  $P$  and  $T$  in our proof. For instance, to check the triangle inequality, we compose the transport maps  $T$  and also compose  $P$  by a matrix multiplication: Given  $P: X \times Y \rightarrow \mathbb{R}$  and  $Q: Y \times Z \rightarrow \mathbb{R}$ , we take  $\frac{1}{M} \sum_{y \in Y} P(x, y) Q(y, z): X \times Z \rightarrow \mathbb{R}$ . The calculations in each step are similar to, but more intricate than, the calculations in the Wasserstein distance proof.  $\square$

Because  $\Delta(X, Y)$  is a metric, it can be adapted into many applications that require metric spaces, for instance constructions for approximate nearest neighbor search (Andoni et al., 2018).

#### 3.2. Global information: spectral vs metric

The COPT metric and GW metric are both optimal transport metrics for graphs. The main difference between them is in what information about the graph they emphasize. The GW distance is defined in terms of the metric  $d_X$ , and so it measures primarily changes to the graph that change the distance function by a large amount, while COPT is defined in terms of  $L_X^\dagger$ , so it measures primarily changes to the graph that change the eigenvectors of the Laplacian with small eigenvalue by a large amount.

To see the difference between these two concepts, consider a graph with two clusters. The distance between a point in the first cluster and a point in the second cluster is determined mainly by the *length of the shortest path* between the clusters. Adding new paths between the clusters will not change the distance much, while lengthening all paths will change the distance drastically. On the other hand, the entries of the matrix  $L_X^\dagger$  with row in the first cluster and column between the cluster is determined more by the *number of paths* between these clusters. As we add more and more paths, these entries of  $L_X^\dagger$  will get less and less negative, up until the number of paths between the clusters is almost as

large as the number of paths within a cluster. On the other hand, lengthening the paths will affect  $L_X^\dagger$  less.

To see the relationship between the graph Laplacian and counting short paths, it is convenient to use the formula

$$L_X^{-1} = (D_X - A_X)^{-1} =$$

$$D_X^{-1} + D_X^{-1}A_XD_X^{-1} + D_X^{-1}A_XD_X^{-1}A_XD_X^{-1} + \dots$$

where  $A_X$  is the adjacency matrix and  $D_X$  is a diagonal matrix whose diagonal entries are the degrees of each vertex. Thus, each entry of the graph Laplacian is a formal series counting paths. (As long as  $X$  is connected and not bipartite, this sum converges once we orthogonally project each term onto the complement of the all 1s matrix, as doing this removes the influence of the all 1s eigenvector.)

Because both metric and spectral information are likely relevant to a practical problem about graphs, it should often be helpful to combine the GW and coordinated optimal transport distances. The combined distance could be seen as similar to the definition by (Vayer et al., 2019) of a distance between graphs with extra structure, except that the “extra structure” is the graph signal and thus is determined by the shape of the graph. We demonstrate experimentally that combining the two indeed boosts classification accuracies.

#### 4. COPT for graph sketching

Using our distance function between graphs, we define a method to sketch a graph by reducing it to a low-dimensional matrix, i.e. the sketched Laplacian. The sketched Laplacian preserves key spectral information about the graph. We then attack classification problems for graphs by applying algorithms such as nearest neighbor search to the sketched Laplacians, which is more computationally efficient than applying it to the full graph.

**Motivation.** Consider a graph  $X$  on  $N$  vertices and a number  $M$ . We could search for the graph  $Y$  on  $M$  vertices that minimizes our distance function  $\Delta(X, Y)$ . In theory, this graph would be the  $M$ -vertex graph that best approximates  $X$ , and therefore should share many of the same features (e.g. clusters or the lack thereof), but with fewer vertices. If we have a large number of graphs  $X_1, \dots, X_n$  to compare, rather than computing the pairwise distances, it would be faster to reduce each to a smaller graph  $Y_1, \dots, Y_n$  and compute the pairwise distances of the  $Y_i$ .

**Method.** However, there are two problems with reducing to a smaller graph: 1) this is a discrete optimization problem, and continuous optimization problems are computationally simpler; 2) the number of isomorphism classes of graphs on a small vertex set is relatively small, so smaller graphs cannot preserve much information.

---

#### Algorithm 1 COPT graph sketching

---

**Input:** Graph  $X$ , size  $N$

**Input:** Target sketch dimension  $M$

**Initialize:**  $L_X^\dagger \leftarrow$  inverse Laplacian of  $X$

**Initialize:**  $(L_Y)'$  for the  $M(M-1)/2$  strict upper triangular entries of  $L_Y$ , drawn from the standard Gaussian

**Initialize:**  $P(x, y)$  for  $x \in X, y \in Y$ , sampled from Uniform(1, 2)

**for**  $i = 1$  **to** `n_iter` **do**

**Set**  $P(x, y) = \text{abs}(P(x, y))$

**Normalize**  $P(x, y)$  by 5 iterations of Sinkhorn-Knopp algorithm

**Ensure Laplacianness:** for  $y_1 < y_2$ ,  $(L_Y)_{y_2 y_1} \leftarrow -(L_Y)_{y_1 y_2}^2$ ,  $(L_Y)_{y_1 y_2} \leftarrow (L_Y)_{y_2 y_1}$ ,  $(L_Y)_{y_1 y_1} \leftarrow -\sum_{y_2 \neq y_1} L_{y_1 y_2}$

**Minimize** objective Eq (5):

**I:** Compute gradient of Eq (7) evaluated at  $L_Y$  and  $P(x, y)$

**II:** Update  $L_Y'$  and  $P(x, y)$  using gradient

**end for**

**Return:**  $L_Y, P(x, y)$

---

The solution to both these difficulties is to relax the question. Our distance function depends only on the Laplacian  $L_Y$  of  $Y$ . Rather than finding the graph that minimizes the distance, we find the Laplacian  $L_Y$  that minimizes the distance. We choose  $L_Y$  subject to the conditions typical of a Laplacian matrix - it is symmetric, its off-diagonal entries are nonpositive, and its row and column sums vanish. Alternatively, we can view this as finding the weighted graph  $Y$  whose distance to  $X$ , defined using the weighted Laplacian, is minimized.

Formally, the sketch of the graph  $X$  is given by the  $L_Y$  which attains the minimum

$$\min_{L_Y \in M_Y(\mathbb{R})} \min_{\substack{P: X \times Y \rightarrow \mathbb{R}^+ \\ (L_Y)_{y_1 y_2} = (L_Y)_{y_2 y_1} \\ (L_Y)_{y_1 y_2} \leq 0 \text{ if } y_1 \neq y_2 \\ \sum_{y_2} L_{y_1 y_2} = 0}} \sum_{x \in X} P(x, y) = N \quad (8)$$

$$M \text{tr}(L_X^\dagger) + N \text{tr}(L_Y^\dagger) - 2 \text{tr}(((L_Y^\dagger)^{1/2} P^T L_X^\dagger P (L_Y^\dagger)^{1/2})^{1/2})$$

In practice, we use a gradient descent algorithm on both  $P$  and  $L_Y$  simultaneously to find an approximate minimum.

##### 4.1. Implementation

As summarized in Algorithm 1, the values of the transport plan  $P$  are initially uniformly sampled from the interval  $[1, 2]$ . At the beginning of each iteration, we normalize  $P$  so its row and column sums are equal, by using the Sinkhorn-Knopp algorithm (Cuturi, 2013). This ensures that  $P$  is a transport plan.

$L'_Y$  corresponds to the upper triangular part of  $L_Y$ , as that entirely determines the Laplacian.  $L'_Y$  is initialized from the standard Gaussian. At the start of each iteration,  $L_Y$  is obtained by taking its upper triangular part to be  $-(L'_Y)^2$ , then symmetrized, and diagonal terms filled, to ensure it's a Laplacian matrix.

Gradient descent is used to minimize the analytic formulation Eq (7), where  $L'_Y$  and  $P$  are updated at each step, with the Adam optimizer (Kingma & Ba, 2015) with a multistep learning rate scheduler that reduces the learning rate multiplicatively at regular intervals. When using COPT to determine the distance between two graphs with Laplacians  $L_X$  and  $L_Y$ , only  $P$  is optimized over in each iteration. Our implementation uses PyTorch and one P100 GPU, on a 2.60GHz six-core Intel CPU machine.

As sanity checks, we confirm that 1) the sketched Laplacian  $L_Y$  converges to the original graph's Laplacian  $L_X$  when the target sketch dimension is that of the original graph, and 2) the distance converges to 0 when  $L_X$  and  $L_Y$  are fixed to be equal. The effects of  $P$  as a transport plan can be seen from the node labels in sketched graphs in Figure 5.4.

Because our sketching algorithm can be used to reduce graphs of varying size to vectors of fixed size, it allows many downstream tasks to be performed efficiently on GPUs, which are well-adapted to performing many similar computations but slow at logic and branching. Algorithms that take advantage of the sparsity of graph adjacency matrices rarely perform well on GPUs because these typically involve branching. Thus, our sketching algorithm which transforms a large sparse matrix into a smaller dense matrix leads to another efficiency boost.

## 4.2. Time complexity

We estimate the coordinated optimal transport distance by a gradient descent algorithm. The time complexity is given by (number of iterations  $\times$  time to calculate each iteration). We are unaware of a general method to estimate the number of iterations needed to converge (in practice  $\sim 150$  iterations suffice to sketch 50-node to 15-node graphs, and  $\sim 1000$  iterations to sketch 1000-node to 200-node graphs), so we focus on estimating the time per iteration, which essentially consists of evaluating

$$M \operatorname{tr}(L_X^\dagger) + N \operatorname{tr}(L_Y^\dagger) - 2 \operatorname{tr}(((L_Y^\dagger)^{1/2} P^T L_X^\dagger P (L_Y^\dagger)^{1/2})^{1/2})$$

and its derivative with respect to  $P$ . This can be done in matrix multiplication time  $\max(N, M)^\omega$ . To see this, note that computing the inverse of a matrix can be done in matrix multiplication time, and that these pseudoinverses can be computed by orthogonally projecting onto the complement of the all 1s vector and then taking a usual inverse. Furthermore, the trace of the square root of a matrix is the sum of the square roots of the eigenvalues, and the eigenvalues can

be computed in matrix multiplication time (Pan & Chen, 1999), noting that we do not need the most computationally difficult step (c) as we only need the eigenvalues and not the eigenvectors. Using backpropagation, computing the gradient has the same time complexity as computing the function.

For graph optimal transport, the time complexity per iteration is similar, but a greater number of iterations are needed to converge in our experiments.

## 4.3. Relations of our reduction algorithm to prior work

We can analogize this approach to other areas where a complicated discrete object is reduced to a vector in a small-dimensional, but semantically rich, vector space. For instance, latent semantic analysis (LSA) (Deerwester et al., 1990) reduces both words and texts consisting of many words to elements of some vector space  $\mathbb{R}^n$ . This is done by a singular value decomposition, which can also be viewed as a minimization problem - minimizing the mean squared error of the prediction of the number of occurrences of a given word in a given text by the dot products of their associated vectors. LSA preserves the most important dimensions of linguistic variation between words and texts. Analogously, COPT preserves the most important dimensions of combinatorial and spectral variation between graphs, by solving an appropriate minimization problem.

A similar graph sketching problem was studied by (Garg & Jakkola, 2019). Their solution also uses an optimal transport approach but is otherwise very different. Rather than compressing a graph  $X$  to a general graph  $Y$ , they specifically forced  $Y$  to be a subgraph of  $X$  with at most a given number of vertices. Because of this, they defined their optimal transport function directly in terms of the distance on  $X$ . They thus chose to find the probability distribution on the vertices of  $X$ , with at most a given number of vertices in its support, that minimizes the Wasserstein distance to the uniform distribution on  $X$ . Like the GW distance, this approach preserves largely metric, rather than spectral, information on graphs.

## 5. Experiments

COPT can be used both for sketching when given one graph, and finding the distance when given two graphs. Here we demonstrate its effectiveness on a variety of tasks: retrieval, classification, summarization, and visualization. Additional experiments on comparison with GOT and with state-of-the-art graph compression techniques can be found in the supplementary material.

We work with connected, undirected graphs. The ‘‘connected’’ assumption is unnecessary, but we focus on connected graphs as they are more relevant for most applica-

tions. The “undirected” assumption is necessary because we define the variance-covariance matrix of  $\mu^X$  as the pseudoinverse of the Laplacian. A variance-covariance matrix is always symmetric, so the Laplacian must be symmetric.

### 5.1. Graph Retrieval

Here we test the quality of COPT sketches by graph retrieval quality. Since there is not an objective nearest neighbor for graphs amongst the randomly generated graphs, retrieval quality is judged by accuracy of the class of the nearest neighbor.

Here we take the dataset  $\{G_X\}$  and queries  $\{G_Q\}$  to be 600 and 180 randomly generated 50-node graphs, respectively, each evenly distributed amongst six classes: random geometric (Penrose, 2003), block-2<sup>1</sup>, block-3, block-4 (Holland et al., 1983), Barabasi-Albert (Barabási & Albert, 1999), and random regular graphs (Steger & Wormald, 1999). We vectorize each graph  $G$  in two ways: 1) sketch  $G$  to 15 nodes with COPT, and flattening the upper triangular part of the sketched Laplacian to obtain a 120-dimensional vector<sup>2</sup>, 2) take the spectral projection of  $G$ ’s Laplacian, specifically the eigenvectors corresponding to the three smallest non-zero eigenvalues (the zero eigenvalue corresponds to the constant eigenvector), yielding a 150-dimensional vector. Smallest eigenvalues are taken as the lower spectrum corresponds to global structure.

Given a query graph vector  $v_q$ , we take its predicted class to be the class of its nearest neighbor, where the distance is determined with  $l_1$  distance for COPT sketches, and  $l_2$  for spectral projections. For COPT sketches the  $l_1$  distance slightly outperforms  $l_2$  distance, likely due to a small number of high-degree vertices overshadowing others when using  $l_2$ <sup>3</sup>. Note that the distances between  $v_q$  and the entire dataset are efficiently computed simultaneously using matrix multiplications with broadcasting.

**Canonicalization.** Since the ordering of the nodes per graph is arbitrary, for vector coordinate-wise comparison to make sense, we canonicalize the ordering of the rows by permuting the rows according to the diagonal term on each row, and subsequently permuting columns to preserve symmetry. In other words, nodes are ordered according to their (weighted) degrees. To canonicalize spectral projection vectors, we order the eigenvectors according to their eigenvalues, and order the entries of the eigenvectors (corresponding to nodes) such that the entries of the least eigenvector are in sorted order.

As seen in table 5.1, when taking the nearest one neighbor’s

<sup>1</sup>stochastic block model consisting of two main communities.

<sup>2</sup>even though the diagonal terms are redundant, they improve retrieval accuracy.

<sup>3</sup>for spectral projections  $l_2$  distance yields better accuracy.

	Spectral proj.	COPT	GW
Accuracy	$0.828 \pm .006$	$0.978 \pm .011$	$0.998 \pm .003$
Timing	$2.25 \pm .2$ ms	$1.81 \pm .07$ ms	$3.69 \pm .07$ s

Table 1. NN1-based classification accuracy and timing comparison. Timing is per query on 600 datapoints, averaged over 180 queries and repeated three times.

class as the predicted class, classification accuracy using COPT is .157 points higher on average than using spectral projections, and over  $2000\times$  faster than GW<sup>4</sup>, while only trailing .02 points behind GW in accuracy. This is implemented on CPU to be a fair comparison, vector-based search runs even faster on GPU.

**Combining in pipeline.** In practice, a faster, but coarser, algorithm is often used to filter out candidates for a more accurate but time-consuming method, so we report accuracies for pipelines combining COPT and spectral projections with GW, respectively, where the fast algorithm is allowed to filter out candidates. This experiment is repeated three times.

As seen in table 5.1, retrieval using sketched Laplacians significantly outperforms spectral projections of original Laplacians, despite requiring 30 fewer coordinates per data point.

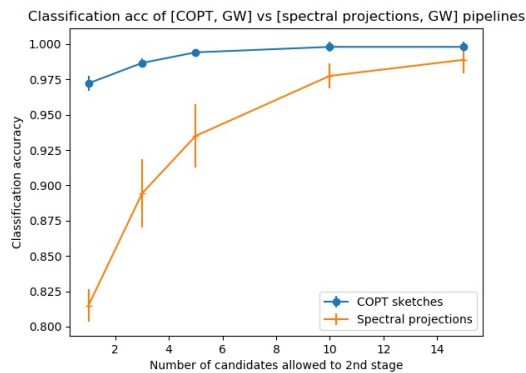


Figure 1. Comparing nearest-neighbor based classification between using COPT sketches and spectral projections of graphs.

### 5.2. COPT + GW

To illustrate that COPT preserves a different kind of global structure as GW, as explained in section §3.2, we compare classification accuracy on COPT sketches to accuracy on the original graphs using GW. Specifically, the search dataset  $\{G_X\}$  consists of six classes, same as in section §5.1, of randomly generated 50-node graphs, with 15 graphs per class for a total of 90 graphs. The query set  $\{G_Q\}$  consists of 60 randomly generated graphs evenly split across the

<sup>4</sup>As implemented in (Vayer et al., 2019).

same six classes. We then apply COPT on  $\{G_X\}$  and  $\{G_Q\}$  to construct 15-node sketches  $\{S_X\}$  and  $\{S_Q\}$ , respectively.

Classifications predictions are based on the classes of nearest neighbors, using the COPT metric between the 15-node graphs  $\{S_Q\}$  and  $\{S_X\}$ <sup>5</sup>, compared with using GW between the original 50-node graphs  $\{G_Q\}$  and  $\{G_X\}$ .

Given a query, the predicted class is the class with the largest representation amongst the 10 nearest neighbors. We found this voting scheme to boost classification accuracy for both graph sketches and GW, over using the nearest neighbor’s class as the prediction. The number of COPT iterations for graph sketching is capped at 230, and during distance computations is capped at 150 for experimental agility.

This experiment is repeated 15 times. As seen in Figure 5.2, we found that COPT + GW combined consistently outperforms either sketch distance or GW alone, substantiating the theoretical justification in section 3.2 that the two preserve different kinds of global structures that complement each other.

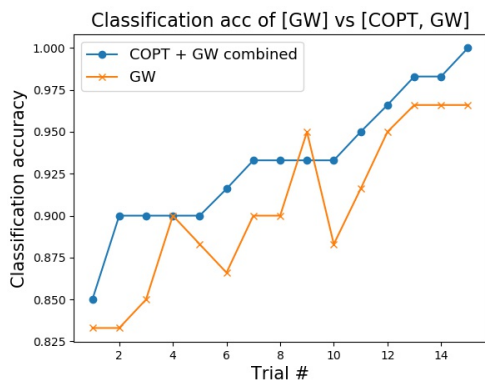


Figure 2. Comparison of classification accuracy between GW and COPT + GW combined over 15 trials. Trials sorted by accuracy for clarity.

### 5.3. Graph projection to low dimensions

Projecting graphs to low dimensions can be an effective technique for visualizing relations amongst graphs, analogous to how projection techniques such as t-SNE (van der Maaten & Hinton, 2008) can yield important insights in the distribution of data points.

Here a set of 80 ten-node graphs consisting evenly of four classes of graphs<sup>6</sup>: 2-block (Holland et al., 1983), random regular (Steger & Wormald, 1999), powerlaw tree, and cave-man (Watts, 1999), are sketched down to graphs on three nodes, and the three entries in the strict upper triangular

<sup>5</sup>Done by fixing  $L_y$  (in addition to  $L_x$ ) in Algorithm 1.

<sup>6</sup>These classes were chosen as they admit meaningfully distinct properties on ten nodes, unlike for instance a four-community graph.

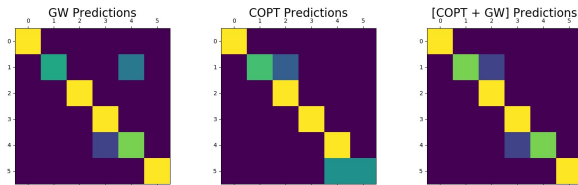


Figure 3. Confusion matrices of nearest-neighbors based classification on 50-node graphs. Accuracies: COPT: 0.87, GW: 0.9, COPT + GW combined: 0.93. COPT refers to applying COPT to sketch the 50-node graphs to 15-node graphs first, and then using the COPT distance to determine the nearest neighbors. GW distances are computed on the original 50-node graphs. The trend of the combined method exhibiting higher accuracy is consistent across trials, indicating that spectral and metric global information complement each other as described in §3.2.

part of the sketched Laplacian are *canonicalized* by sorting, and used as three-dimensional vector representations of the graphs.

As seen in Figure 5.3 and the zoomed in version, the 3D sketches of each class of graphs roughly follow the same trend, whether clustering together or lying in some consistent subspace.

### 5.4. Graph Summarization

Figures 5.4 visually demonstrate that COPT preserves the most relevant global structures on graphs, across graphs of varying structures. The sketched graphs are obtained from Algorithm 1 by declaring an entry in the sketched Laplacian  $L_y$  an edge if it lies above a given threshold. The node labels on the sketched graphs are determined using the transport plan  $P$ , specifically the label on a node contains the two top-weighted nodes in the original graph whose mass flowed into that node. This shows that 1) COPT preserves important global graph structures, and 2) structurally similar nodes in the original graph are sketched to the same or nearby nodes. See supplementary material for more examples.

## 6. Conclusion

We introduced a novel distance metric between graphs and optimization routine, computing a coordinated pair of optimal transport maps simultaneously. This is an unsupervised way to learn general-purpose graph representations. COPT preserves important global spectral structure on graphs, improving upon and complementing state of the art methods such as the GW distance. COPT is well-suited for tasks on graphs including retrieval, classification, summarization, and visualization.

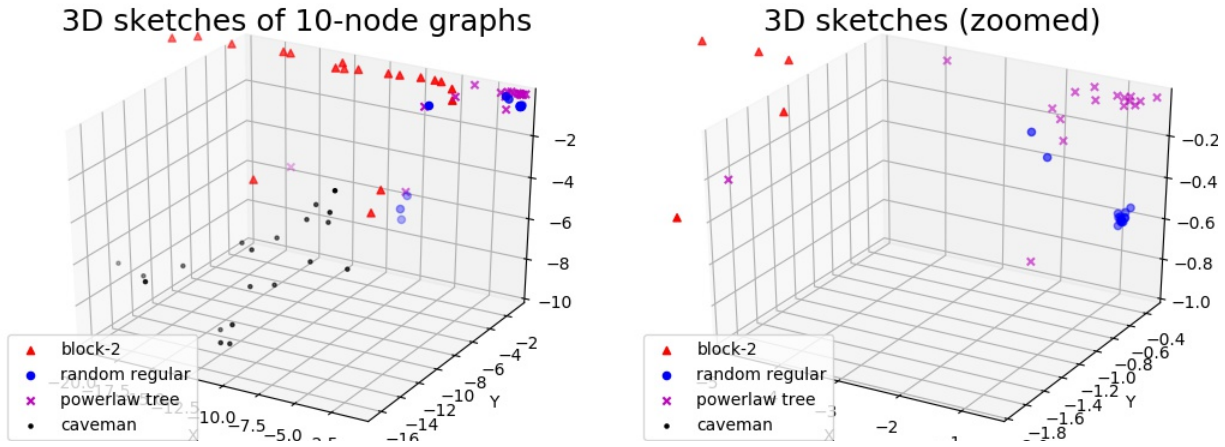


Figure 4. 3D sketches of 80 ten-node graphs (left) and zoomed in version (right) reveal that sketches of the same class cluster together or lie in the same subspace.

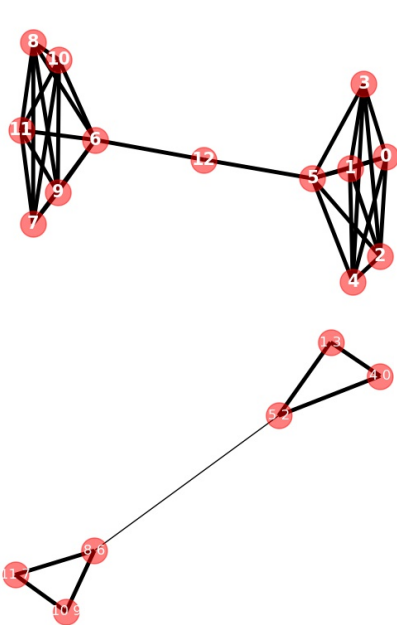


Figure 5. Barbell.

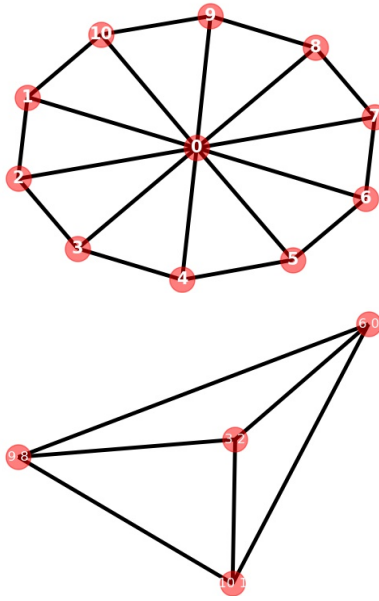


Figure 6. Wheel.

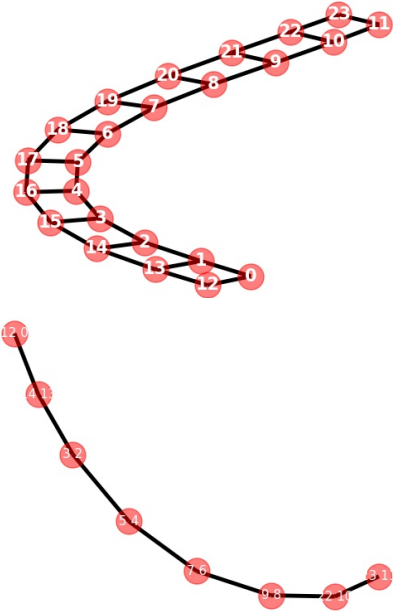


Figure 7. Ladder.

Figure 8. Original graphs (top) and their sketched graphs. The node labels on the sketched graphs are determined using the transport plan  $P$ , specifically the label on a node contains the two top-weighted nodes in the original graph whose mass flowed into that node. COPT sketches structurally similar nodes in the original graph to the same or nearby nodes.



## 7. Acknowledgments

This research was conducted during the period Will Sawin served as a Clay Research Fellow.

## References

- Alvarez-Melis, D. and Jaakkola, T. S. Gromov-Wasserstein alignment of word embedding spaces. *arXiv:1809.00013*, 2018.
- Andoni, A., Indyk, P., and Razenshteyn, I. Approximate nearest neighbor search in high dimensions. *arXiv preprint arXiv:1806.09823*, 2018.
- Barabási, A. L. and Albert, R. Emergence of scaling in random networks. *Science*, 286:509–512, 1999.
- Bravo-Hermsdorff, G. and Gunderson, L. M. A unifying framework for spectrum-preserving graph sparsification and coarsening. *arXiv:1902.09702*, 2019.
- Chen, J. and Safro, I. Algebraic distance on graphs. *SIAM Journal on Scientific Computing*, 33(6):3468–3490, 2011.
- Cuturi, M. Sinkhorn distances: Lightspeed computation of optimal transport. In *Advances in neural information processing systems*, pp. 2292–2300, 2013.
- D. I. Shuman, M. J. F. and Vandergheynst, P. A multiscale pyramid transform for graph signals. *IEEE Transactions on Signal Processing*, 64(8):2119–2134, 2016.
- Dai, H., D. B. and Song, L. Discriminative embeddings of latent variable models for structured data. In *ICML’16: Proceedings of the 33rd International Conference on International Conference on Machine Learning*, pp. 2702–2711, 2016.
- Deerwester, S., Dumais, S. T., Furnas, G. W., Landauer, T. K., and Harshman, R. Indexing by latent semantic analysis. *Journal of the American Society for Information Science*, 41(6):391–407, 1990. doi: 10.1002/(SICI)1097-4571(199009)41:6<391::AID-ASII>3.0.CO;2-9. CiteSeerX 10.1.1.108.8490.
- Defferrard, M., Bresson, X., and Vandergheynst, P. Convolutional neural networks on graphs with fast localized spectral filtering. In *Advances in Neural Information Processing Systems*, pp. 3844–3852, 2016.
- Dhillon, I., Guan, Y., and Kulis, B. Weighted graph cuts without eigenvectors a multilevel approach. In *IEEE transactions on pattern analysis and machine intelligence*, volume 29(11), pp. 1944–1957, 2007.
- Dong, X., Thanou, D., Rabbat, M., and Frossard, P. Learning graphs from data: a signal representation perspective. *IEEE Signal Processing*, 2019. *arXiv:1806.00848*.
- Dörfler, F. and Bullo, F. Kron reduction of graphs with applications to electrical networks. *IEEE Transactions on Circuits and Systems I: Regular Papers*, 60(1):150–163, 2013.
- Garg, V. K. and Jakkola, T. Solving graph compression via optimal transport. In *33rd Conference on Neural Information Processing Systems (NeurIPS 2019)*, 2019.
- Holland, P. W., Laskey, K. B., and Leinhardt, S. Stochastic blockmodels: First steps. *Probability and Computing*, 5: 109–137, 1983.
- Jin, Y., Loukas, A., and Jaja, J. Graph coarsening with preserved spectral properties. *arXiv:1802.04447*, 2019.
- Kantorovich, L. V. On translation of mass (in russian). *Proceedings of the USSR Academy of Sciences*, 37:199–201, 1942.
- Karypis, G. and Kumar, V. A fast and high quality multilevel scheme for partitioning irregular graphs. *SIAM Journal on Scientific Computing*, 20(1):359–392, 1998.
- Kingma, D. and Ba, J. Adam: A method for stochastic optimization. In *International Conference for Learning Representations*, 2015.
- Livne, O. E. and Brandt, A. Lean algebraic multigrid (LAMG): Fast graph Laplacian linear solver. *SIAM Journal on Scientific Computing*, 34(4):B499–B522, 2012.
- Loukas, A. Graph reduction with spectral and cut guarantees. *Journal of Machine Learning Research*, 20(116):1–42, 2019.
- Loukas, A. and Vandergheynst, P. Spectrally approximating large graphs with smaller graphs. In *International Conference on Machine Learning (ICML)*, 2018.
- Maretic, H. P., Gheche, M. E., Chierchia, G., and Frossard, P. GOT: An optimal transport framework for graph comparison. In *33rd Conference on Neural Information Processing Systems (NeurIPS)*, 2019.
- Mémoli, F. Gromov-Wasserstein distances and the metric approach to object matching. *Foundations of Computational Mathematics*, 11:418–487, 2011.
- Pan, V. Y. and Chen, Z. Q. The complexity of the matrix eigenproblem. In *Proceedings of the Thirty-First Annual ACM Symposium on Theory of Computing, STOC ’99*, pp. 507–516, New York, NY, USA, 1999. Association for Computing Machinery. ISBN 1581130678. doi: 10.1145/301250.301389. URL <https://doi.org/10.1145/301250.301389>.
- Penrose, M. Random geometric graphs. *Oxford Studies in Probability*, 5, 2003.

- Peyré, G., Cutri, M., and Solomon, J. Gromov-Wasserstein averaging of kernel and distance matrices. In *ICML'16: Proceedings of the 33rd International Conference on International Conference on Machine Learning*, volume 48, pp. 2664–2672, 2016.
- Ron, D., Safro, I., and Brandt, A. Relaxation-based coarsening and multiscale graph organization. *Multiscale Modeling & Simulation*, 9(1):407–423, 2011.
- Rue, H. and Held, L. *Gaussian Markov random fields: theory and applications*. Chapman and Hall, 2005.
- Steger, A. and Wormald, N. Emergence of scaling in random networks. *Probability and Computing*, 8:377–396, 1999.
- Sturm, K. On the geometry of metric measure spaces. *Acta Mathematica*, 196(1):65–131, 2006.
- Takatsu, A. Wasserstein geometry of Gaussian measures. In *Osaka Journal of Mathematics*, volume 48, pp. 1005–1026, 2011.
- Tsitsulin, A., Mottin, D., Karras, P., Bronstein, A., , and Muller, E. NetLSD: hearing the shape of a graph. In *Proceedings of the 24th ACM SIGKDD International Conference on Knowledge Discovery & Data Mining*, pp. 2347–2356. ACM, 2018.
- van der Maaten, L. J. P. and Hinton, G. E. Visualizing data using t-sne. *Journal of Machine Learning Research*, 9: 2579–2605, 2008.
- Vayer, T., Chapel, L., Flamery, R., Tavenard, R., and Courty, N. Optimal transport for structured data with application on graphs. arXiv:1805.09114, 2019.
- Von Luxburg, U. A tutorial on spectral clustering. *statistics and computing*. *SIAM Journal on scientific Computing*, 17(4):395–416, 2007.
- Watts, D. J. Networks, dynamics, and the small-world phenomenon. *Amer. J. Soc.*, 105:493–527, 1999.
- Yanardag, P. and Vishwanathan, S. Deep graph kernels. In *Proceedings of the 21th ACM SIGKDD International Conference on Knowledge Discovery & Data Mining*, pp. 1365–1374. ACM, 2015.

## 8. Appendix Outline

In this supplement, we give full proofs of Lemmas 3.1 and 3.2, further discuss COPT optimizations during training, as well as give additional experimental results on graph summarization, training progress, and comparison between COPT and GOT, including both theoretical and empirical results that GOT is a special case of COPT when  $N = M$ , finally, we evaluate COPT sketching quality by comparing with state-of-the-art graph compression techniques on the commonly-benchmarked dataset MUTAG (Yanardag & Vishwanathan, 2015).

## 9. Full proofs to lemmas

We give full proofs to Lemma 3.1, an analytic formula for the COPT metric, and Lemma 3.2, the statement that COPT is a metric.

**Lemma 9.1** (Lemma 3.1). *Let  $X$  and  $Y$  be graphs with vertices sets of size  $N$  and  $M$  respectively. Then*

$$\begin{aligned} & \inf_{\substack{T: \mathbb{R}^X \rightarrow \mathbb{R}^Y \\ T_{\#} \mu^X = \mu^Y}} \int_{\mathbb{R}^X} \sum_{x \in X} \sum_{y \in Y} (f(x) - Tf(y))^2 P(x, y) d\mu^X(f) \\ &= M \operatorname{tr}(L_X^\dagger) + N \operatorname{tr}(L_Y^\dagger) - 2 \operatorname{tr}(((L_Y^\dagger)^{1/2} P^T L_X^\dagger P (L_Y^\dagger)^{1/2})^{1/2}) \end{aligned}$$

where  $P$  is the matrix with entries  $P(x, y)$ .

*Proof.* Let  $A$  be the map from  $\mathbb{R}^X$  to  $\mathbb{R}^{X \times Y}$  that sends a function  $f$  on  $X$  to the function  $f(x) \sqrt{P(x, y)}$  on  $X \times Y$ . Similarly, let  $B$  be the map from  $\mathbb{R}^Y$  to  $\mathbb{R}^{X \times Y}$  that sends a function  $f$  to  $f(y) \sqrt{P(x, y)}$ . Then the distance between  $A(f)$  and  $B(T(f))$  in  $\mathbb{R}^{X \times Y}$  is

$$\sum_{x \in X} \sum_{y \in Y} (f(x) \sqrt{P(x, y)} - Tf(y) \sqrt{P(x, y)})^2 = \sum_{x \in X} \sum_{y \in Y} (f(x) - Tf(y))^2 P(x, y).$$

Thus, we can interpret this minimum as the Wasserstein distance between the pushforward  $A_{\#} \mu^X$  of  $\mu^X$  along  $A$  and the pushforward  $B_{\#} \mu^Y$  of  $\mu^Y$  along  $B$ . Because  $A$  and  $B$  are linear maps, these distributions are both multivariate Gaussians with mean zero. Thus, we can use the formula for the Wasserstein distance between multivariate Gaussians with mean zero, which is expressed in terms of their covariance matrices (Takatsu, 2011, Theorem 2.2 and Remark 4.2). The formula is

$$\operatorname{tr}(V(A_{\#} \mu^X)) + \operatorname{tr}(V(B_{\#} \mu^Y)) - 2 \operatorname{tr} \left( \left( V(A_{\#} \mu^X)^{1/2} V(B_{\#} \mu^Y) V(A_{\#} \mu^X)^{1/2} \right)^{1/2} \right).$$

We have

$$V(A_{\#} \mu^X) = AL_X^\dagger A^T$$

and

$$V(B_{\#} \mu^Y) = BL_Y^\dagger B^T$$

and we have by direct calculation

$$A^T A = MI_N,$$

$$B^T B = NI_M,$$

$$B^T A = P,$$

$$A^T B = P^T,$$

giving

$$\operatorname{tr}(V(A_{\#} \mu^X)) = \operatorname{tr}(AL_X^\dagger A^T) = \operatorname{tr}(L_X^\dagger A^T A) = M \operatorname{tr}(L_X^\dagger)$$

$$\operatorname{tr}(V(B_{\#} \mu^Y)) = \operatorname{tr}(BL_Y^\dagger B^T) = \operatorname{tr}(L_Y^\dagger B^T B) = N \operatorname{tr}(L_Y^\dagger)$$

For the last term, it is convenient to define the trace of the square root of a matrix as the sum of the square roots of its eigenvalues, so that it can be defined for more than just symmetric positive definite matrices, allowing us to write

$$\begin{aligned} \operatorname{tr} \left( \left( V(A_{\#}\mu^X)^{1/2} V(B_{\#}\mu^Y) V(A_{\#}\mu^X)^{1/2} \right)^{1/2} \right) &= \operatorname{tr} \left( (V(A_{\#}\mu^X) V(B_{\#}\mu^Y) V)^{1/2} \right) \\ &= \operatorname{tr} \left( \left( AL_X^\dagger A^T BL_Y^\dagger B^T \right)^{1/2} \right) = \operatorname{tr} \left( \left( B^T AL_X^\dagger A^T BL_Y^\dagger \right)^{1/2} \right) \\ &= \operatorname{tr} \left( \left( PL_X^\dagger P^T L_Y^\dagger \right)^{1/2} \right) = \operatorname{tr} \left( \left( (L_Y^\dagger)^{1/2} PL_X^\dagger P^T (L_Y^\dagger)^{1/2} \right)^{1/2} \right). \end{aligned}$$

Combining these, we get exactly the stated formula. Note that, in our final formula, the matrix is again semidefinite, so we can take a canonical square root.  $\square$

**Lemma 9.2** (Lemma 3.2).  $\Delta(X, Y)$  is a metric on the set of isomorphism classes of finite graphs.

*Proof.* If  $X = Y$  then the distance is 0, because then  $L_X = L_Y$  and we can take  $P$  to be the diagonal matrix  $NI_N$ .

Conversely, let us check that if the distance is zero then  $X = Y$ . Because the distance is the minimum of a continuous function over the compact set of possible values of  $P$ , if the distance is zero then zero is obtained for a particular value of  $P$ . Because the Wasserstein distance between two distributions is zero if and only if they are the same distribution, it follows that (in the notation of the previous lemma)  $AL_X^\dagger A^T = BL_Y^\dagger B^T$ , which in concrete terms means that

$$\left( L_X^\dagger \right)_{x_1 x_2} = \left( L_Y^\dagger \right)_{y_1 y_2}$$

whenever  $P(x_1, y_1) \neq 0$  and  $P(x_2, y_2) \neq 0$ . Taking  $y_1 = y_2 = y$ , this implies

$$\left( L_X^\dagger \right)_{x_1 x_2} = \left( L_X^\dagger \right)_{x_1 x_1}$$

whenever  $P(x_1, y) \neq 0$  and  $P(x_2, y) \neq 0$ . This identity implies  $x_1 = x_2$ , because the unique maximum of a column of  $L_X^\dagger$  is on the diagonal. Thus, we see that  $P(x, y) \neq 0$  for a unique  $x$  for each  $y$ . By symmetry this must also be true for a unique  $y$  for each  $x$ . Because  $P(x, y) \neq 0$  for at least one  $y$  for each  $x$ , and at least one  $x$  for each  $y$ , the set where  $P(x, y) \neq 0$  defines a permutation. After applying that permutation, our identity can be written

$$L_X^\dagger = L_Y^\dagger$$

which implies

$$L_X = L_Y$$

and thus

$$X = Y.$$

Symmetry is easiest to check using Lemma 3.1 and the fact that the trace of the square root of a matrix, like the trace of a matrix, is invariant under cyclic permutations, so

$$\begin{aligned} \operatorname{tr} \left( \left( (L_Y^\dagger)^{1/2} P^T L_X^\dagger P (L_Y^\dagger)^{1/2} \right)^{1/2} \right) &= \operatorname{tr} \left( \left( (L_Y^\dagger)^{1/2} P^T (L_X^\dagger)^{1/2} (L_X^\dagger)^{1/2} P (L_Y^\dagger)^{1/2} \right)^{1/2} \right) \\ &= \operatorname{tr} \left( \left( (L_X^\dagger)^{1/2} P (L_Y^\dagger)^{1/2} (L_Y^\dagger)^{1/2} P^T (L_X^\dagger)^{1/2} \right)^{1/2} \right) = \operatorname{tr} \left( \left( (L_X^\dagger)^{1/2} P L_Y^\dagger P^T (L_X^\dagger)^{1/2} \right)^{1/2} \right) \end{aligned}$$

so swapping  $P$  and  $P^T$ , our formulas for the two distances are equal.

Finally, we check the triangle inequality. Let  $X, Y$ , and  $Z$  be graphs with  $|X| = N$ ,  $|Y| = M$ , and  $|Z| = L$ . Let  $P$  and  $T$  satisfy the conditions in the definition of  $\Delta(X, Y)$  so that the integral is within  $\epsilon$  of the minimum value. Similarly let  $Q$  and  $S$  satisfy the conditions in the definition of  $\Delta(Y, Z)$ . It suffices to show that

$$\left( \frac{1}{MN} \int_{\mathbb{R}^X} \sum_{x \in X} \sum_{y \in Y} (f(x) - Tf(y))^2 P(x, y) d\mu^X(f) \right)^{1/2} \quad (9)$$

$$\begin{aligned}
 & + \left( \frac{1}{NL} \int_{\mathbb{R}^Y} \sum_{y \in Y} \sum_{z \in Z} (f(y) - Sf(z))^2 Q(y, z) d\mu^Y(f) \right)^{1/2} \\
 & \geq \left( \frac{1}{ML} \int_{\mathbb{R}^X} \sum_{x \in X} \sum_{z \in Z} (f(x) - STf(z))^2 \sum_{y \in Y} \frac{P(x, y) Q(y, z)}{N} d\mu^X(f) \right)^{1/2}.
 \end{aligned}$$

because then  $\sum_{y \in Y} \frac{P(x, y) Q(y, z)}{N}$  and  $S \circ T$  satisfy the conditions in the definition of  $\Delta(X, Z)$ , and then taking  $\epsilon$  sufficiently small, we obtain the triangle inequality.

This inequality follows from the Cauchy-Schwarz inequality

$$\left( \frac{1}{MNL} \int_{\mathbb{R}^X} \sum_{x \in X} \sum_{y \in Y} \sum_{z \in Z} (f(x) - STf(z))^2 P(x, y) Q(y, z) d\mu^X(f) \right)^{1/2} \leq \quad (10)$$

$$\left( \frac{1}{MNL} \int_{\mathbb{R}^X} \sum_{x \in X} \sum_{y \in Y} \sum_{z \in Z} (f(x) - Tf(y))^2 P(x, y) Q(y, z) d\mu^X(f) \right)^{1/2} \quad (11)$$

$$+ \left( \frac{1}{MNL} \int_{\mathbb{R}^X} \sum_{x \in X} \sum_{y \in Y} \sum_{z \in Z} (Tf(y) - STf(z))^2 P(x, y) Q(y, z) d\mu^X(f) \right)^{1/2} \quad (12)$$

where (11) simplifies to the first term of (9) by using  $\sum_{z \in Z} Q(y, z) = L$  and (12) simplifies to the second term of (9) by using  $\sum_{x \in X} P(x, y) = N$  and  $T_{\#}\mu_X = \mu_Y$  so the integral against  $\mu_X$  of a function of  $Tf$  is equal to the integral against  $\mu_Y$  of the same function of  $f$ .

□

## 10. Further details on COPT optimization

Here we elaborate further on COPT's optimization routine. As the objective Equation 3.1 is not globally convex, gradient descent can fall into local minima. To facilitate faster convergence towards global minima, we use a combination of learning rate scheduling and a learning rate hikes.

Specifically, the learning rate is initialized at 0.4. During training, it's scaled multiplicatively by 0.7 per 100 iterations. Once the *change* in loss drops below a threshold, set at 0.002 throughout, for 10 different iterations, the learning rate is increased five-fold, capped at 4.0. If an upper bound on the number of iterations is set, learning rate hikes stop 200 iterations before the max number of iterations, to allow convergence. These parameters can be tuned with respect to the downstream task, we have found COPT to be robust with respect to the parametrizations.

Figure 10 illustrates the effects learning rate hikes on training loss, where LR hiking is the only difference between the two curves. The loss increases briefly when the learning rate is hiked, but can soon drop below the level had there been no hikes. LR hiking not only improves convergence rate, but experiments show it also changes the final transport plan  $P$ , indicating convergence to a better minimum.

We observe that this optimization routine allows for **faster runtime** per iteration than stochastic exploration used in GOT, which, to avoid converging to local minima, uses a stochastic exploration method that minimizes the *expectation* of the distance (Equation 4), rather than the distance itself. But this requires many random explorations at each step to achieve good performance.

For instance, when aligning the same set of 50-node graphs, on the same machine and CPU, 1000 iterations of GOT takes  $18.8 \pm 0.72$  seconds, and COPT takes  $3.18 \pm 0.59$  seconds, with settings that were tuned to produce the best community discovery results for each method, which as observed are commensurable (see Section §11 for details). This is repeated 20 times.

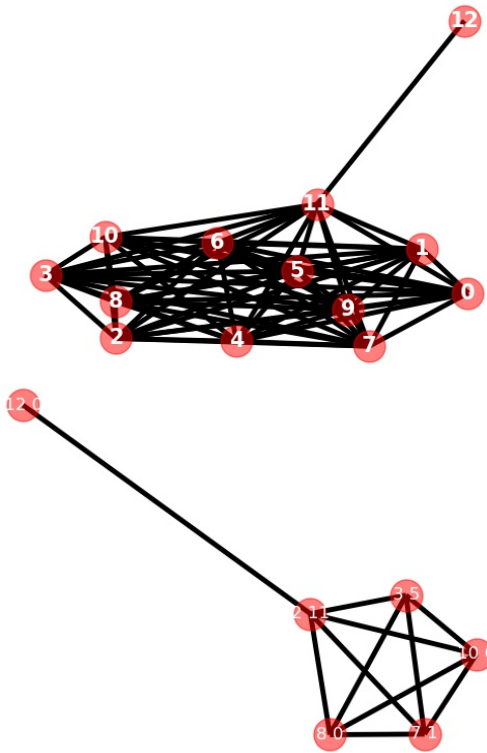


Figure 9. Lollipop.

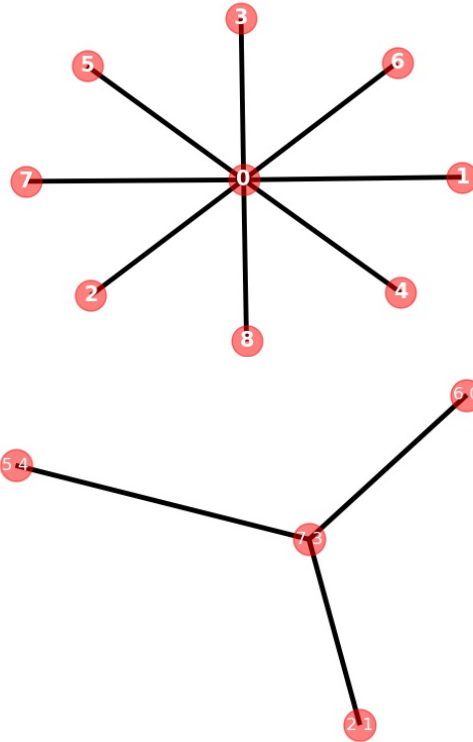


Figure 10. Star.

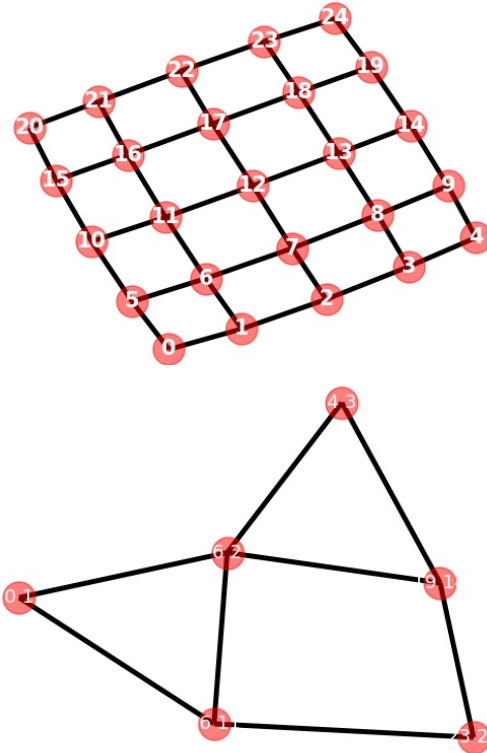


Figure 11. Grid.

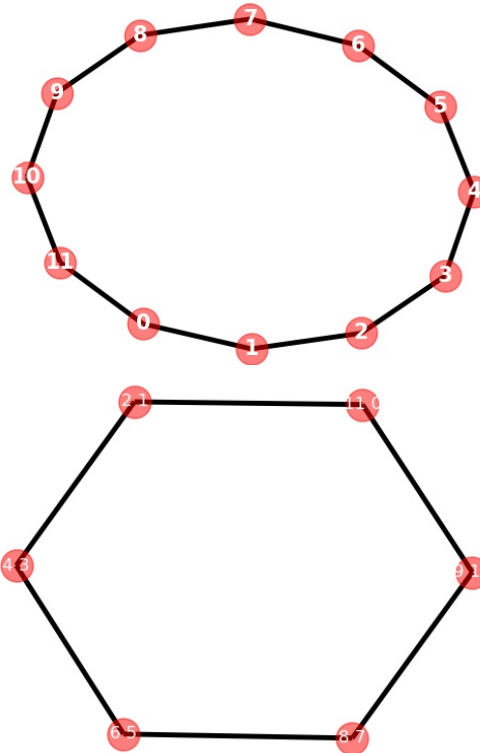


Figure 12. Ring.

Figure 13. **Graph summarization:** original graphs (above) and their sketched graphs (below). The node labels on the sketched graphs are determined using the transport plan  $P$ , specifically the label on a node contains the two top-weighted nodes in the original graph whose mass flowed into that node. COPT sketches structurally similar nodes in the original graph to the same or nearby nodes.

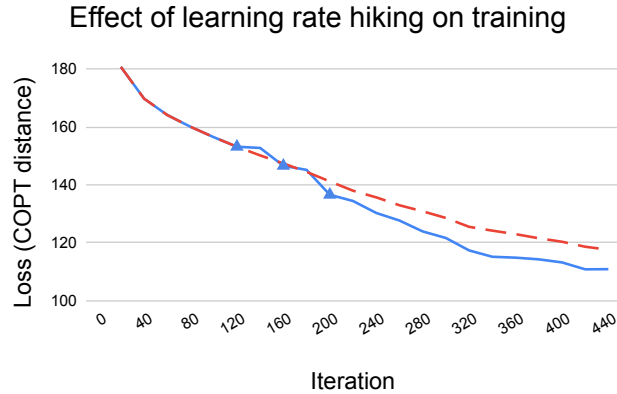


Figure 14. The impact of learning rate (LR) spiking on COPT training, in this case computing the alignment and distance between two 25-node graphs. The dashed line represents no LR hiking, the solid line represents LR hiking, the triangles indicate LR hikes. The hikes are triggered when the change in loss falls below 0.002 over 10 different iterations. Not only are the rates of convergence different, the two converge to different permutations.

## 11. Further comparison with GOT

Under the special case  $N = M$ , because the transport plan  $P$  converges to a permutation, COPT reduces to the GOT metric described in (Maretic et al., 2019). We prove this in Lemma 12.1. As this case uses the same optimization backbone when  $N \neq M$  as well as for sketching, COPT and GOT differ in their implementations.

We want to compare the methods in the special case  $N = M$ , to ensure that, as in theory, the two implementations are commensurable.

However, the permutations between the two in the alignment task are not directly comparable, as many graphs carry symmetries that allow multiple transport plans to achieve the same objective minimum<sup>7</sup>.

Thus, to compare our implementation with GOT’s, we repeat one key alignment experiment in (Maretic et al., 2019), where 40-node four-community graphs are aligned with corrupted and permuted versions of themselves, and the alignment quality is measured using the normalized mutual information (NMI).

Specifically, we 1) randomly delete a given number of nodes, 2) permute nodes in the reduced graphs, 3) align between the original graphs and the permuted reduced graphs using COPT and GOT, and 4) compare the resulting NMI using the permutations produced by the alignment algorithms.

As shown in Table 11, the NMI are commensurable. Each measurement is repeated 20 times after parameter tuning. Furthermore, the GOT NMI are consistent with (Maretic et al., 2019), which also report that these NMI scores outperform the NMI for the same evaluation settings using GW.

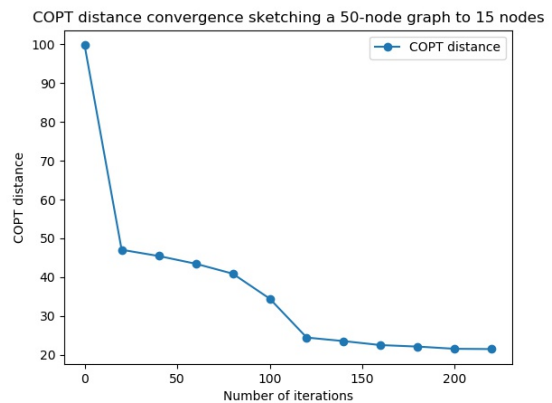


Figure 15. Sketching a 50-node graph down to 15 nodes with COPT, which typically converges in  $\sim 200$  iterations.

<sup>7</sup>Inspection by hand reveals that, on “simple” graphs such as two-block graphs, the transport plans produced by COPT and GOT are the same up to symmetry.

## Coordinated Optimal Transport

#Edges rem.	30	60	90	120	150	180	210	240
GOT	.997 ± .013	1 ± 0	.991 ± .022	.960 ± .059	.837 ± .092	.855 ± .10	.844 ± .096	.862 ± .11
COPT	1 ± 0	1 ± 0	.994 ± .026	.964 ± .094	.873 ± .13	.848 ± .13	.897 ± .125	.871 ± .14

*Table 2. Alignment quality as gauged by community discovery performance.* Normalized mutual information (NMI) scores between 40-node graphs against corrupted and then permuted versions of themselves, using GOT and COPT implementations. Higher is better. First row indicates number of edges removed. The same upper bound on the number of iterations, 1000, is used for both methods, and parameters tuned. GOT is a special case of COPT when  $N = M$ , and the NMI above demonstrates that they are also commensurable empirically.

## 12. Characterization of minima

The following lemma characterizes the minima in the COPT objective function, in general and in the special case  $N = M$ .

**Lemma 12.1.** *Any local, hence global, minimum of the function*

$$\inf_{\substack{T: \mathbb{R}^X \rightarrow \mathbb{R}^Y \\ T_{\#} \mu^X = \mu^Y}} \int_{\mathbb{R}^X} \sum_{x \in X} \sum_{y \in Y} (f(x) - Tf(y))^2 P(x, y) d\mu^X(f)$$

on the convex polyhedron

$$\left\{ P : X \times Y \rightarrow \mathbb{R}^+ \mid \sum_{x \in X} P(x, y) = N, \sum_{y \in Y} P(x, y) = M \right\}$$

that is isolated, in the sense that no other point within distance  $\epsilon$  for any  $\epsilon$  is a local minimum, is a vertex of that polyhedron.

In particular, if  $N = M$ , every isolated local minimum is a permutation matrix.

Because local minima being isolated is a generic condition, this shows that the local minima are permutations away from a set of Laplacians  $L_X, L_Y$  with measure 0, and thus COPT will converge to a permutation outside a set of measure 0.

*Proof.* Let  $P_0$  be a local minimum of

$$\inf_{\substack{T: \mathbb{R}^X \rightarrow \mathbb{R}^Y \\ T_{\#} \mu^X = \mu^Y}} \int_{\mathbb{R}^X} \sum_{x \in X} \sum_{y \in Y} (f(x) - Tf(y))^2 P(x, y) d\mu^X(f) = \min_{\gamma} L(P, \gamma)$$

where the minimum is taken over measures  $\gamma$  on  $\mathbb{R}^X \times \mathbb{R}^Y$  whose projection to  $\mathbb{R}^X$  is  $\mu^X$  and whose projection to  $\mathbb{R}^Y$  is  $\mu^Y$ , and where

$$L(P, \gamma) = \int_{\mathbb{R}^X} \int_{\mathbb{R}^Y} \sum_{x \in X} \sum_{y \in Y} (f(x) - g(y))^2 P(x, y) d\gamma(f, g).$$

We switch from the transport map to the joint measure formulation of optimal transport as only for the joint measure is the minimum always attained.

Let  $\gamma_0$  be the value of  $\gamma$  which attains this minimum. Thus  $P_0$  is also a local minimum of  $L(P, \gamma_0)$ . To prove this, note that if  $L(P, \gamma_0)$  a smaller value at some nearby point,  $\min_{\gamma} L(P, \gamma)$  a smaller value, because  $\gamma_0$  is included in the minimum over  $\gamma$ , and so  $P_0$  will fail to be a local minimum of  $\min_{\gamma} L(P, \gamma)$  assumed.

Because  $L(P, \gamma_0)$  is a linear function of  $P$ , its local minima are simply faces of the polyhedron of possible values of  $P$ . If  $P$  is not a vertex, then it lies in a positive-dimensional face, on which  $L(P, \gamma_0)$  is constant, and thus on which every value of  $\min_{\gamma} L(P, \gamma)$  is at most  $L(P_0, \gamma_0) = \min_{\gamma} L(P, \gamma)$ . In this situation, the only way  $P_0$  can be a local minimum of  $\min_{\gamma} L(P, \gamma)$  is if  $\min_{\gamma} L(P, \gamma)$  is actually constant on a neighborhood of  $P_0$  in this face. In that case, every point in the constant region is a local minimum, contradicting our assumption that  $P$  is a local minimum.

Finally, we must check that every vertex if  $N = M$  corresponds to a permutation. To see this, let  $P$  be a vertex, and consider a bipartite graph with vertices  $X \cup Y$  with an edge connecting  $x \in X$  and  $y \in Y$  if and only if  $P(x, y) \neq 0$ .



Compression	METIS -*	EM -*	LV -*	SGC -*	SC -*	MGC -*	COPT- $l_1$	COPT-*
Class. Acc.	.776	.789	.790	.803	.804	.815	.833	.854

Table 3. NN1-based classification accuracy on MUTAG with different compression methods, where graphs are reduced to  $1/5$  as many nodes. -\* indicates using NetLSD to compute distances between reduced graphs, and  $-l_1$  indicates using  $l_1$  distance between the upper triangular parts of the sketched Laplacians. The evaluation is done with 10-fold cross validation on the dataset.

Let us check that this graph does not contain any cycle. If it did, because the graph is bipartite, we could 2-color each edge of the cycle. Then for any sufficiently small  $\epsilon > 0$ , raising  $P(x, y)$  by  $\epsilon$  for  $(x, y)$  each red edge and lowering  $P(x, y)$  by  $\epsilon$  for  $(x, y)$  each blue edge would preserve all the conditions on  $P$  defining the polyhedron. Similarly, lowering  $P(x, y)$  for the red edges and raising  $P(x, y)$  for the blue edges would preserve the condition. Thus  $P(x, y)$  is a convex combination of two different points in the polyhedron and hence is not a vertex.

Because this graph does not contain a cycle, all its connected components must be trees, and every tree contains a leaf. But if  $x \in X$  is a leaf, then  $P(x, y) > 0$  for a unique  $y$ , so  $P(x, y) = M = N$  and thus  $P(x', y) = 0$  for a unique  $x'$ . The same holds if  $y \in Y$  is a leaf. Thus every leaf is connected to another leaf and so every tree is a single edge, so in fact every component of the graph is a single edge. Thus, each  $x \in X$  is connected by exactly one edge to a unique  $y \in Y$ , and vice

versa, defining a permutation  $\sigma : X \rightarrow Y$  with  $P(x, y) = \begin{cases} N & y = \sigma(x) \\ 0 & y \neq \sigma(x) \end{cases}$ .

□

### 13. Comparison with graph compression techniques

We evaluate COPT sketching quality by comparing with state-of-the-art graph compression techniques, on the task of classifying graphs in the commonly-benchmarked dataset MUTAG (Yanardag & Vishwanathan, 2015).

MUTAG is a nitro compounds dataset divided into two classes depending on mutagenic activity, it consists of 188 graphs and averages 17.93 nodes per graph. All methods compared reduce the number of nodes five-fold.

We compare with the techniques spectral clustering (SC) (Von Luxburg, 2007), a commonly used graph clustering technique using the eigenvectors of the Laplacian; METIS (Karypis & Kumar, 1998), a multi-level graph partitioning algorithm; edge matching (EM) (Dhillon et al., 2007; Defferrard et al., 2016), a coarsening algorithm based on maximum weight matching; local variation (LV) (Loukas & Vandergheynst, 2018; Loukas, 2019), a neighborhood-based method, spectral graph clustering (SGC) (Jin et al., 2019), which generalizes graph clustering by combining with  $k$ -means clustering; and multilevel graph coarsening (MGC) (Jin et al., 2019), a coarsening algorithm that iteratively merges nodes with similar normalized edge weights. The results on these methods are from (Jin et al., 2019), which has the exact same experimental setup. As in prior work (Dai & Song, 2016; Tsitsulin et al., 2018), task evaluation is done with 10-fold cross validation on the dataset.

NetLSD (Tsitsulin et al., 2018) is used to compute distances between reduced graphs for all techniques, by deriving a heat trace signature on each reduced graph. In addition, we also compare COPT-reduced graphs by using  $l_1$  distance between the upper triangular parts of the sketched Laplacians<sup>8</sup> as in Section §5.1, as it is simple and computationally efficient and hence easily adaptable. Given these distances, the predicted class of a query is that of its nearest neighbor.

As shown in Table 13, COPT sketching outperforms existing compression methods in classification accuracy, even when the distance between sketched graphs is simply the  $l_1$  distance between sketched Laplacians. One of COPT’s strengths is that, during sketching, the mass of one node is able to flow to multiple nodes in the compressed graph.

<sup>8</sup>padded to achieve uniform size.